HHS Public Access

Author manuscript

Cell Signal. Author manuscript; available in PMC 2015 April 22.

Published in final edited form as:

Cell Signal. 2014 September ; 26(9): 1818–1824. doi:10.1016/j.cellsig.2014.04.018.

Early NADPH oxidase-2 activation is crucial in phenylephrine-induced hypertrophy of H9c2 cells

Nynke E. Hahn[a,f], **René J.P. Musters**[b,f], **Jan M. Fritz**[a], **Patrick J. Pagano**[e], **Alexander B.A. Vonk**[c,f], **Walter J. Paulus**[b,f], **Albert C. van Rossum**[d,f], **Christof Meischl**[a,f], **Hans W.M. Niessen**[a,c,f], and **Paul A.J. Krijnen**[a,f,*]

[a]Department of Pathology, VU University Medical Center, Amsterdam, The Netherlands
[b]Department of Physiology, VU University Medical Center, Amsterdam, The Netherlands
[c]Department of Cardiac Surgery, VU University Medical Center, Amsterdam, The Netherlands
[d]Department of Cardiology, VU University Medical Center, Amsterdam, The Netherlands
[e]Department of Pharmacology and Chemical Biology, Vascular Medicine Institute, University of Pittsburgh, Pittsburgh, PA, USA [f]ICaR-VU, Institute for Cardiovascular Research, VU University Medical Center, Amsterdam, The Netherlands

Abstract

Reactive oxygen species (ROS) produced by different NADPH oxidases (NOX) play a role in cardiomyocyte hypertrophy induced by different stimuli, such as angiotensin II and pressure overload. However, the role of the specific NOX isoforms in phenylephrine (PE)-induced cardiomyocyte hypertrophy is unknown. Therefore we aimed to determine the involvement of the NOX isoforms NOX1, NOX2 and NOX4 in PE-induced cardiomyocyte hypertrophy. Hereto rat neonatal cardiomyoblasts (H9c2 cells) were incubated with 100 μM PE to induce hypertrophy

*Corresponding author at: VU University Medical Center, Department of Pathology, De Boelelaan 1117, 1007 MB Amsterdam, The Netherlands. Tel.: +31 20 444 4003., paj.krijnen@vumc.nl (P.A.J. Krijnen).

Disclosures

No conflict of interest exists regarding the contents of this manuscript.

Contributions

Nynke E. Hahn	design and analysis of all data, writing and approval
René J.P. Musters	design and analysis of digital fluorescence microscopy, critical revising and approval
Jan M. Fritz	design and analysis of electron microscopy, critical revising and approval
Patrick J. Pagano	critical revising and approval
Alexander B.A. Vonk	critical revising and approval
Walter J. Paulus	critical revising and approval
Albert C. van Rossum	critical revising and approval
Christof Meischl	design and analysis of all data, critical revising and approval
Hans W.M. Niessen	design and analysis of all data, critical revising and approval
Paul A.J. Krijnen	design and analysis of all data, writing and approval

after 24 and 48 h as determined via cell and nuclear size measurements using digital imaging microscopy, electron microscopy and an automated cell counter. Digital-imaging microscopy further revealed that in contrast to NOX1 and NOX4, NOX2 expression increased significantly up to 4 h after PE stimulation, coinciding and co-localizing with ROS production in the cytoplasm as well as the nucleus. Furthermore, inhibition of NOX-mediated ROS production with apocynin, diphenylene iodonium (DPI) or NOX2 docking sequence (Nox2ds)-tat peptide during these first 4 h of PE stimulation significantly inhibited PE-induced hypertrophy of H9c2 cells, both after 24 and 48 h of PE stimulation. These data show that early NOX2-mediated ROS production is crucial in PE-induced hypertrophy of H9c2 cells.

Keywords

Cardiomyocyte hypertrophy; Phenylephrine; NADPH oxidase; NOX2

1. Introduction

Cardiac hypertrophy is a (patho)physiological adaptive response of the heart to pressure overload [1]. However, after prolonged periods, this initial adaptive response may become maladaptive, leading to increased mortality and morbidity from heart failure [2]. Therefore, unraveling the cellular mechanisms underlying cardiomyocyte hypertrophy is crucial for the development of therapeutic strategies to counteract maladaptive cardiac hypertrophy.

Left ventricular hypertrophy can be the result of many pathogenic factors, including hypertension [3]. However, in contrast to pressure overload, angiotensin II was shown to cause cardiac hypertrophy in-vivo, independent of hypertension [4]. The α1-adrenergic receptor agonist phenylephrine (PE) can also induce cardiomyocyte hypertrophy and was shown to be an independent and more effective inducer of cardiomyocyte hypertrophy than angiotensin II [5,6]. These studies underline the different stimulus-dependent pathways regulating cardiomyocyte hypertrophy.

Redox-sensitive mechanisms play an essential role in mediating the development of cardiac hypertrophy, in which NADPH oxidases (NOX) are particularly important [7]. Different NOX isoforms NOX1, NOX2, NOX4, NOX5 and DUOX1/DUOX2 meanwhile have been identified either in cardiomyocytes and/or vascular cells [8–12]. In particular NOX2 and NOX4 were shown to be involved in pro-apoptotic [9,10, 13] but remarkably also pro-hypertrophic [14,15] signaling in cardiomyocytes. Angiotensin II-induced hypertrophy coincided with an increased left ventricular NOX activity that was reduced in NOX2 knock-out mice compared to wild-type controls [16]. In contrast, in a pressure overload model, induced by aortic constriction, identical cardiac hypertrophy was found both in wild-type mice as well as NOX2 knockout mice [16]. In these NOX2 knock-out mice, however, increased NOX4 expression was detected in the left ventricle, whereas NOX1 expression was not found [16]. In cardiac specific NOX4 knock-out mice indeed a decrease in ROS and cardiac hypertrophy was found after aortic constriction. In these NOX4 knock-out mice expression levels of NOX2 were not affected compared to wild-type controls and NOX1 was not found [10].

Tanaka et al. have shown in isolated rat cardiomyocytes that PE induced an increase in ROS generation that was counteracted by the flavoenzyme inhibitor diphenylene iodonium (DPI), pointing to NOX as the ROS source [17]. Albeit, the identity of the NOX isoform(s) involved was not investigated. In addition, increased NOX activity was in heart homogenates of rats treated with PE that coincided with phosphorylation of $p47^{phox}$, although the specific cell type nor the involvement of specific NOX isoforms was studied [18]. Therefore, the role of NOX isoforms in PE-induced cardiomyocyte hypertrophy is unknown. In the present study we aimed to determine the involvement of the NOX isoforms NOX1, NOX2 and NOX4 in PE-induced hypertrophy in H9c2 rat cardiomyoblasts.

2. Materials and methods

2.1. Cell culture

Rat cardiomyoblast cells (H9c2 cells) were obtained from the American Type Culture Collection ((ATCC), Manassas, VA, USA) and cultured in culture medium: Dulbecco's modified eagle's medium (DMEM, Cambrex Corporation, East Rutherford, NJ, USA) with the addition of 10% (v/v) heat inactivated fetal calf serum (FCS, BioWhittaker, Walkersville, MD, ASU), 100 IU/ml penicillin (Yamanouchi Europe BV, Meppel, The Netherlands), 100 μg/ml streptomycin (Radiopharma Fisiopharma, Palomonte, Italy) and 2 mM L-glutamine (Invitrogen Corporation, Carlsbad, CA, USA). H9c2 cells were cultured at a 5% CO_2 atmosphere at 37 °C.

To induce hypertrophy, the cells were starved for 18 h in DMEM containing 1% FCS and subsequently incubated with 100 μM PE (Sigma, Milwaukee, USA) up to 48 h. Different inhibitors of NOX were studied herein, namely apocynin (100 μM, Sigma [19]; an inhibitor of the association of cytosolic and membrane-bound components of NADPH oxidase), DPI (10 μM, Sigma [19]; a flavoenzyme inhibitor) and NOX2 docking sequence tat peptide (Nox2ds-tat: 50 μM [20]; a specific inhibitor of the NOX2).

2.2. Determination of cell size

Digital-imaging microscopy—The area of the cell was determined via quantification of the total surface. To specify between stretching of cells and hypertrophy, the size of the nucleus was determined via both quantification of the square area and its volume via 3D stack images.

Electron microscopy—The cells were fixed in 2% glutaraldehyde for 30 min and 1.5% osmium tetraoxide for 10 min. The cells were then dehydrated with acetone and embedded in Epon 812. Ultrathin sections were collected on 300-mesh Formvar-coated Nickel grids. The sections were contracted with uranyl acetate and lead citrate and were examined in a Jeol-1200 EX electron microscope. Five electron microscopy pictures of control cells or PE-stimulated cells were analyzed to determine the area of the nucleus (magnification 9000×, 5 cells per picture) and the area of the whole cell (magnification 4500×, 10 cells per picture).

Automatic cell counter—The diameter of cells in suspension was quantified with a Scepter 2.0 Handheld Automated Cell Counter (Millipore, Billerica, MA, USA) according to standard operating procedure.

2.3. Digital-imaging microscopy

After treatment, H9c2 cells were fixed with 4% paraformaldehyde for 10 min at 37 °C and permeabilized with acetone–methanol (30%–70% (v/v)) for 10 min at RT. The cells were subsequently incubated with the primary antibodies for 1 h at RT followed by incubation overnight at 4 °C. Primary antibodies used were goat-anti NOX1 (1:50, Santa Cruz, CA, USA), rabbit-anti $p91^{phox}$ (NOX2: 1:50, Upstate, North Billerica, MA, USA) and goat-anti NOX4 (1:50, Santa Cruz). The cells were then incubated with the secondary antibodies Alexa Fluor 568-labeled donkey-anti goat (1:40, Invitrogen) and Alexa Fluor 647-labeled donkey-anti rabbit (1:40, Invitrogen) for 30 min at RT in the dark. Negative controls with only secondary antibody were included to assess nonspecific binding. These controls were all negative (data not shown). Before visualization, mounting medium containing 4′,6-diamidino-2-phenylindole (DAPI; H-1500, Vector Laboratories Inc., Burlingame, CA, USA) was added and the cells were covered.

2D/3D optical sections were acquired and analyzed with a 3I Marianas™ digital-imaging microscopy workstation (Zeiss Axiovert 200 M inverted microscope; Cark Zeiss, Sliedrecht, The Netherlands). Exposures, objectives and pixel binning were automatically recorded with each image. Data processing was controlled by Slidebook™ software (version 4.2; Intelligent Imaging Innovations, Denver, CO, USA). Expression levels of NOX1, NOX2 and NOX4 were determined via quantification of the mean intensity.

2.4. Imaging of ROS production

H9c2 cells were cultured in chamber slides and after treatment either fixed and stained with rabbit-anti nitrotyrosine (1:50, Invitrogen), as an indirect marker of ROS generation [21] (1:50, Invitrogen) or loaded with 10 μM 5-(*6*)-chloromethyl-2′,7′-dichlorodihydrofluorescein diacetate acetyl ester (CM-H_2DCFDA), as a marker of H_2O_2 generation (Molecular Probes, Leiden, The Netherlands). As described above, the cells were analyzed by the use of 3I Marianas™ digital-imaging microscopy workstation. The cells were scored by determining the number of nitrotyrosine/H_2O_2-positive H9c2 cells.

2.5. Detection of caspase 3 activity

Caspase 3 activity in H9c2 cells was measured using a caspase 3 assay kit (Homogenous caspase 3/7 assay kit, Roche, Mannheim, Germany). Equal cell numbers were lysed and incubated with DEVD-rhodamine 110 substrate (Roche, Mannheim, Germany) for one hour at 37 °C. The amount of free rhodamine was determined using a micro-plate fluorescence reader (TECAN SpectraFluor, Switzerland) with an absorption filter of 492 λ, an emission filter of 535 λ and a gain of 93.

2.6. Statistics

The SPSS statistics program (Windows version 9.0) was used for statistical analysis. To evaluate whether observed differences were significant, the paired *T*-test and one-way ANOVA with post hoc Bonferroni test were used. In the relevant figures and in the text values are given as mean ± SE. A two-sided p value of 0.05 or less was considered to be significant.

3. Results

3.1. Phenylephrine induces hypertrophy in H9c2 cells

PE-induced hypertrophy in attached H9c2 cells was analyzed using digital-imaging microscopy. Stimulation with PE for 1, 2, 4, 8 and 16 h induced a non-significant increase in cell area with 7 ± 4%, 30 ± 7%, 27 ± 3%, 20 ± 3% and 11 ± 3% respectively, compared to control cells (Fig. 1A). Only after 24 and 48 h of PE stimulation a significant increase in cell area was induced, respectively with 52 ± 8% ($p < 0.001$) and 56 ± 5% ($p < 0.001$), compared to control cells. Stimulation with PE for 48 h also significantly increased the size of the nucleus (Fig. 1B, arrows) with 12 ± 4% ($p < 0.05$), compared to control cells (Fig. 1B, graph).

This PE-induced hypertrophy was verified in H9c2 cells in suspension, since attached cells as analyzed above can stretch, thus mimicking hypertrophy. Electron microscopy analysis of these cells showed a significant increase in total cell area (with 36 ± 11%, $p < 0.04$, Fig. 1C–I) and nuclear area (with 72 ± 25%, $p < 0.03$, Fig. 1C–II) after 48 h of PE stimulation. In addition, a significant increase in cell diameter was found (with 19 ± 6%, $p < 0.005$, Fig. 1C–III) as measured via the Automated Cell Counter.

These results thus show that PE induced hypertrophy of H9c2 cells.

3.2. Inhibition of NOX-mediated ROS generation counteracts phenylephrine-induced hypertrophy in H9c2 cells

To verify whether NOX-mediated ROS generation plays a role in PE-induced cardiomyocyte hypertrophy [15,22,23], the effect of the NOX inhibitors apocynin, DPI [19] and Nox2ds-tat [20] on PE-induced hypertrophy was analyzed in attached H9c2 cells using digital-imaging microscopy.

Apocynin, DPI and Nox2ds-tat significantly inhibited the PE-induced increase in cell area with 25 ± 5% (apocynin, $p < 0.01$), 30 ± 4% (DPI, $p < 0.01$) and 46 ± 7% (Nox2ds-tat, $p < 0.01$) after 24 h and with 51 ± 4% (apocynin, $p < 0.001$), 37 ± 4% (DPI, $p < 0.001$) and 35 ± 7% (Nox2ds-tat, $p < 0.001$) after 48 h (Fig. 2A). Although the mechanisms of inhibition of apocynin, DPI and Nox2ds-tat differ [24], no significant differences in their effect on PE-induced hypertrophy were found.

These results thus prove a role for NOX-mediated ROS production in PE-induced cardiomyocyte hypertrophy and point to the involvement of the NOX2 isoform herein.

3.3. Increased NOX2 expression and ROS generation coincide and colocalize in H9c2 cells early after phenylephrine stimulation

Next, the expression levels and subcellular localization of the main NOX isoforms expressed in the heart, e.g. NOX1, NOX2 and NOX4 [25], were analyzed in H9c2 cells at different time points after PE stimulation, using digital-imaging microscopy. Albeit, we have shown NOX5 to be expressed in the human heart [26], NOX5 is not expressed in rodents and was therefore excluded in these analyses.

Neither the expression levels nor the subcellular localization of NOX1 (Fig. 2B and C–I) and NOX4 (Fig. 2B and C–III) was affected by PE stimulation up to 48 h. In contrast, compared to control cells NOX2 expression levels were significantly increased 1, 2 and 4 h after PE stimulation with 50 ± 6% (*$p < 0.001$), 69 ± 6% (*$p < 0.001$) and 40 ± 5% (*$p < 0.001$) respectively (Fig. 2B). After 8 h up to 48 h of PE stimulation NOX2 expression levels were reduced back to control levels. In control cells NOX2 expression was found in the cytoplasm and (peri)nuclear regions (Fig. 2B–II). PE did not induce a difference in the subcellular localization of NOX2.

We subsequently analyzed whether this PE-induced increase in NOX2 expression coincided and colocalized in time with the generation of ROS, measured both via nitrotyrosine expression and H_2O_2 (CM-H_2DCFDA fluorescence). PE increased the expression levels of nitrotyrosine after 1, 2, 4 and 24 h, respectively with 110 ± 67%, 237 ± 31%, 140 ± 42% and 84 ± 44% (Fig. 3A), although this was significant only after 2 h (*$p < 0.01$). In line herewith, PE increased H_2O_2 levels after 1, 2 and 4 h, respectively with 40 ± 25%, 200 ± 71% and 100 ± 25% (Fig. 3B), which again was significant only after 2 h (*$p < 0.01$). After 24 h H_2O_2 expression levels were reduced significantly, to even below control levels with 180 ± 13% ($p < 0.001$). Similar to NOX2, ROS generation was found in the cytoplasm and (peri)nuclear regions of control H9c2 cells (Fig. 3B–I and 3B–II). Also here PE did not induce any differences in the subcellular localization of both nitrotyrosine and H_2O_2. In addition, NOX2 was found to colocalize in the (peri)nuclear region with nitrotyrosine (Fig. 3C–IV, yellow signal) and with DAPI (Fig. 3C–V, white signal), pointing to PE-induced (peri)nuclear NOX2 activity.

(Peri)nuclear NOX2-mediated ROS generation has been shown to play an important role in the induction of apoptosis in H9c2 cells, in response to ischemia [19,27] and homocysteine [13,28]. To analyze whether the PE-induced (peri)nuclear NOX2 expression and ROS generation in (peri)nuclear regions were also related to apoptosis, we measured caspase 3 activity. We found no significant differences in active caspase 3 concentration after 1, 2, 4, 8, 16, 24 or 48 h of PE stimulation compared to control cells (data not shown).

These data thus indicate that early after PE stimulation an increase in NOX2 expression and activity is induced in H9c2 cells.

3.4. Early inhibition of NOX2-mediated ROS generation decreases phenylephrine-induced hypertrophy in H9c2 cells

To prove whether this early NOX2 activation indeed is crucial in PE-induced hypertrophy, we studied the effect of early inhibition of NOX/ROS hereon. For this, apocynin, DPI or Nox2ds-tat was added during the first 4 h only of the 24 hour PE stimulation.

Early inhibition of NOX activity significantly decreased PE-induced increase in total cell area with 44 ± 7% (apocynin, $p < 0.001$), 47 ± 6% (DPI, $p < 0.001$) and 79 ± 6% (Nox2ds-tat, $p < 0.001$) after 24 h and with 67 ± 6% (apocynin, $p < 0.001$), 80 ± 5% (DPI, $p < 0.001$) and 101 ± 5% (Nox2ds-tat, $p < 0.001$) after 48 h, compared to PE stimulation alone (Fig. 4). No significant differences in the effect of the different inhibitors on PE-induced hypertrophy

were found, although only Nox2ds-tat completely counteracted the hypertrophic effects of PE.

Thus, early activation (during the first 4 h) of NOX-mediated ROS generation is crucial in PE-induced hypertrophy of H9c2 cells.

4. Discussion

ROS are important mediators of cardiac hypertrophy. Interestingly, different hypertrophic stimuli (e.g. angiotensin II, pressure overload and PE) were shown to exert their hypertrophic effects via different intracellular signal transduction cascades [4,29,6], suggesting stimuli-specific responses. Moreover, a NOX isoform-specific role herein was suggested, at least in angiotensin II and pressure overload induced hypertrophy [30,16,15,10]. Knowledge of the involvement of the different NOX isoforms in PE-induced cardiac hypertrophy, however, still is lacking. We now found that the isoform NOX2 is crucial in PE-induced hypertrophy of H9c2 cells. Indeed, induction of a hypertrophic phenotype in H9c2 cells 24 and 48 h after PE stimulation depended critically on an increase in NOX2-related ROS generation after 2 h.

Increased NOX activity in response to PE-induced hypertrophy was shown before in rat heart homogenates, although neither the involvement of specific NOX isoforms herein was specified, nor whether this increase in NOX activity was related to cardiomyocytes in particular [18]. We now found that the NOX inhibitors apocynin and DPI inhibited PE-induced hypertrophy of H9c2 cells, underlining the role of NOX herein. Moreover, the inhibitory effect of Nox2ds-tat on PE-induced hypertrophy does point to a role of NOX2 herein. Although, DPI and apocynin do not differentiate between the different NOX isoforms [24], Nox2ds-tat was shown to specifically inhibit NOX2-mediated ROS production, as it mimics a sequence in the cytosolic B-loop of NOX2 that is not present in NOX1 and NOX4 [20]. A role for NOX2 in PE-induced hypertrophy was further supported by the increase in colocalized NOX2 expression and ROS production 2 h after PE stimulation, whereas expression levels of NOX1 and NOX4 did not change. These data strongly point to an important role for NOX2 activity in PE-induced cardiomyocyte hypertrophy. In their study, Isabelle et al. found a PE-induced increase in the phosphorylation of $p47^{phox}$ [18]. As $p47^{phox}$ can activate NOX2 this finding supports our observations in H9c2 cells. Although it has to be noted that $p47^{phox}$ can activate NOX1 as well and that the PE-induced phosphorylation of $p47^{phox}$ was analyzed in rat heart homogenates rather than cardiomyocytes.

As NOX5 is not expressed in rats it is obvious that NOX5 does not play a role in PE-induced hypertrophy in these H9c2 cells. However, as we recently did find NOX5 to be present in human cardiomyocytes [26], we cannot exclude a role of NOX5 in hypertrophy induction in the human heart.

Interestingly, the early NOX2-related ROS generation 2 h after PE stimulation appeared to be crucial for the induction of a hypertrophic phenotype after 24 and 48 h. This corresponds to data found in isolated adult ventricular rat cardiomyocytes wherein elevated levels of intra-cellular ROS were found between 5 and 60 min after PE stimulation, as measured by

oxidation of dichlorofluorescein (DCF) [17]. This generation PE-induced of ROS could be inhibited by DPI. However, a direct effect hereof on hypertrophy nor the involvement of different NOX isoforms herein was studied [17].

This early PE-induced activation of NOX2 we show here in H9c2 cells coincides with extensive activation of early gene expression apparatus in the first hours after PE stimulation in adult rat cardiomyocytes, including ERK1/2, *c-jun* and connective tissue growth factor (CTGF), which after 4 to 24 h is followed by changes in expression of structural genes associated with hypertrophy [31–34]. This is in line with in-vitro findings in mouse myogenic C2C12 cells, showing that angiotensin II induced expression of immediate early genes (e.g. *c-fos*, *c-jun*, and activator protein 1 (AP1)) within 30 min, whereas late markers of cardiac hypertrophy (e.g. skeletal alpha-actin and atrial natriuretic peptide (ANP) expression) were induced after 6 h [35,36]. Also here the involvement of ROS was suggested since ROS scavenger N-acetyl-L-cysteine (NAC) was shown to almost completely abolish the angiotensin II-induced increase of AP1 binding [37]. However, whether the NOX2-related ROS generation we found in this study is causally related to early gene activity and remains to be determined.

In conclusion, our results indicate a time-dependent role of NOX2-mediated ROS production in PE-induced hypertrophy of H9c2 cells.

Acknowledgments

Grants

Supported by a grant from the ICaR-VU (2008V076).

Abbreviations

ANP	atrial natriuretic peptide
AP1	activator protein 1
CTGF	connective tissue growth factor
DCF	dichlorofluorescein
DPI	diphenylene iodonium
gp91ds	gp91 docking sequence
NAC	N-acetyl-L-cysteine
NOX	NADPH oxidase
PE	phenylephrine
ROS	reactive oxygen species

References

1. Tiyyagura SR, Pinney SP. Mt Sinai J Med. 2006; 73:840–851. [PubMed: 17117309]
2. Swynghedauw B. Physiol Rev. 1999; 79:215–262. [PubMed: 9922372]

3. Devereux RB, Roman MJ. Hypertens Res. 1999; 22:1–9. [PubMed: 10221344]
4. Jacobi J, Schlaich MP, Delles C, Schobel HP, Schmieder RE. Am J Hypertens. 1999; 12:418–422. [PubMed: 10232503]
5. Tardiff JC, Hewett TE, Factor SM, Vikstrom KL, Robbins J, Leinwand LA. Am J Physiol Heart Circ Physiol. 2000; 278:H412–H419. [PubMed: 10666070]
6. Zhang TT, Takimoto K, Stewart AF, Zhu C, Levitan ES. Circ Res. 2001; 88:476–482. [PubMed: 11249870]
7. Anilkumar N, Sirker A, Shah AM. Front Biosci. 2009; 14:3168–3187.
8. Cave AC, Brewer AC, Narayanapanicker A, Ray R, Grieve DJ, Walker S, Shah AM. Antioxid Redox Signal. 2006; 8:691–728. [PubMed: 16771662]
9. Krijnen PA, Meischl C, Hack CE, Meijer CJ, Visser CA, Roos D, Niessen HW. J Clin Pathol. 2003; 56:194–199. [PubMed: 12610097]
10. Kuroda J, Ago T, Matsushima S, Zhai P, Schneider MD, Sadoshima J. Proc Natl Acad Sci U S A. 2010; 107:15565–15570. [PubMed: 20713697]
11. Meischl C, Buermans HP, Hazes T, Zuidwijk MJ, Musters RJ, Boer C, van LA, Simonides WS, Blankenstein MA, Dupuy C, Paulus WJ, Hack CE, Ris-Stalpers C, Roos D, Niessen HW. Am J Physiol Cell Physiol. 2008; 294:C1227–C1233. [PubMed: 18322142]
12. Murdoch CE, Zhang M, Cave AC, Shah AM. Cardiovasc Res. 2006; 71:208–215. [PubMed: 16631149]
13. Sipkens JA, Krijnen PA, Meischl C, Cillessen SA, Smulders YM, Smith DE, Giroth CP, Spreeuwenberg MD, Musters RJ, Muller A, Jakobs C, Roos D, Stehouwer CD, Rauwerda JA, van Hinsbergh VW, Niessen HW. Apoptosis. 2007; 12:1407–1418. [PubMed: 17440815]
14. Ago T, Kuroda J, Pain J, Fu C, Li H, Sadoshima J. Circ Res. 2010; 106:1253–1264. [PubMed: 20185797]
15. Hingtgen SD, Tian X, Yang J, Dunlay SM, Peek AS, Wu Y, Sharma RV, Engelhardt JF, Davisson RL. Physiol Genomics. 2006; 26:180–191. [PubMed: 16670255]
16. Byrne JA, Grieve DJ, Bendall JK, Li JM, Gove C, Lambeth JD, Cave AC, Shah AM. Circ Res. 2003; 93:802–805. [PubMed: 14551238]
17. Tanaka K, Honda M, Takabatake T. J Am Coll Cardiol. 2001; 37:676–685. [PubMed: 11216996]
18. Isabelle M, Monteil C, Moritz F, Dautreaux B, Henry JP, Richard V, Mulder P, Thuillez C. Cardiovasc Res. 2005; 67:699–704. [PubMed: 15936005]
19. Hahn NE, Meischl C, Wijnker PJ, Musters RJ, Fornerod M, Janssen HW, Paulus WJ, van Rossum AC, Niessen HW, Krijnen PA. Cell Physiol Biochem. 2011; 27:471–478. [PubMed: 21691064]
20. Csanyi G, Cifuentes-Pagano E, Al Ghouleh I, Ranayhossaini DJ, Egana L, Lopes LR, Jackson HM, Kelley EE, Pagano PJ. Free Radic Biol Med. 2011; 51:1116–1125. [PubMed: 21586323]
21. Duncan MW. Amino Acids. 2003; 25:351–361. [PubMed: 14661096]
22. Liu C, Cao F, Tang QZ, Yan L, Dong YG, Zhu LH, Wang L, Bian ZY, Li H. J Nutr Biochem. 2010; 21:1238–1250. [PubMed: 20185286]
23. Lu YM, Han F, Shioda N, Moriguchi S, Shirasaki Y, Qin ZH, Fukunaga K. Mol Pharmacol. 2009; 75:101–112. [PubMed: 18952768]
24. Jaquet V, Scapozza L, Clark RA, Krause KH, Lambeth JD. Antioxid Redox Signal. 2009; 11:2535–2552. [PubMed: 19309261]
25. Nabeebaccus A, Zhang M, Shah AM. Heart Fail Rev. 2010; 16:5–12. [PubMed: 20658317]
26. Hahn NE, Meischl C, Kawahara T, Musters RJ, Verhoef VM, van d, Vonk AB, Paulus WJ, van Rossum AC, Niessen HW, Krijnen PA. Am J Pathol. 2012; 180:2222–2229. [PubMed: 22503554]
27. Meischl C, Krijnen PA, Sipkens JA, Cillessen SA, Munoz IG, Okroj M, Ramska M, Muller A, Visser CA, Musters RJ, Simonides WS, Hack CE, Roos D, Niessen HW. Apoptosis. 2006; 11:913–921. [PubMed: 16544099]
28. Sipkens JA, Krijnen PA, Hahn NE, Wassink M, Meischl C, Smith DE, Musters RJ, Stehouwer CD, Rauwerda JA, van Hinsbergh VW, Niessen HW. Mol Cell Biochem. 2011; 358:229–239. [PubMed: 21739151]
29. Ruf S, Piper M, Schluter KD. Pflugers Arch. 2002; 443:483–490. [PubMed: 11810220]

30. Bendall JK, Cave AC, Heymes C, Gall N, Shah AM. Circulation. 2002; 105:293–296. [PubMed: 11804982]
31. Amirak E, Fuller SJ, Sugden PH, Clerk A. Biochem J. 2013; 450:351–363. [PubMed: 23215897]
32. Clerk A, Cullingford TE, Fuller SJ, Giraldo A, Markou T, Pikkarainen S, Sugden PH. J Cell Physiol. 2007; 212:311–322. [PubMed: 17450511]
33. Kemp TJ, Aggeli IK, Sugden PH, Clerk A. J Mol Cell Cardiol. 2004; 37:603–606. [PubMed: 15276029]
34. Markou T, Cieslak D, Gaitanaki C, Lazou A. Mol Cell Biochem. 2009; 322:103–112. [PubMed: 19002563]
35. Lijnen P, Petrov V. J Mol Cell Cardiol. 1999; 31:949–970. [PubMed: 10336836]
36. Sadoshima J, Izumo S. Circ Res. 1993; 73:413–423. [PubMed: 8348686]
37. Puri PL, Avantaggiati ML, Burgio VL, Chirillo P, Collepardo D, Natoli G, Balsano C, Levrero M. J Biol Chem. 1995; 270:22129–22134. [PubMed: 7673190]

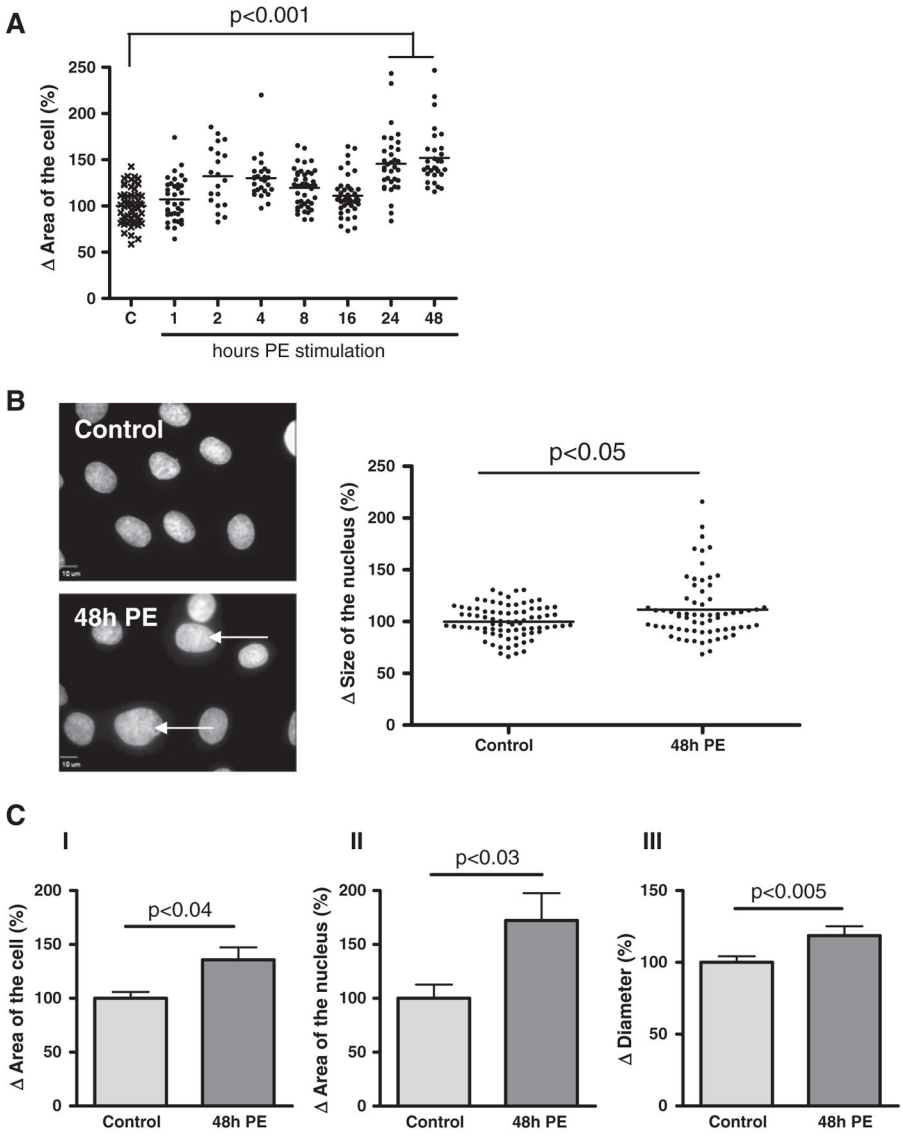

Fig. 1.

Phenylephrine induced hypertrophy of H9c2 cells. Digital-imaging microscopy analysis of phenylephrine (PE)-stimulated H9c2 cells after different time intervals. Analysis of (A) area of the cell (n = 6) and (B) size of the nucleus (n = 4) of attached H9c2 cells. Images of nuclei are stained with DAPI (blue signal), representative for n = 4. Arrows indicate increased area of the nucleus. (C) Analysis of phenylephrine (PE)-stimulated H9c2 cells after 48 h. Electron microscopy analysis of (I) area of the cell (n = 5), (II) area of the nucleus (n = 5) and Automated Cell Counter analysis of (III) diameter (n = 3) of H9c2 cells in suspension. The changes are shown as the difference (Δ) in the percentage compared to control cells set to 100%.

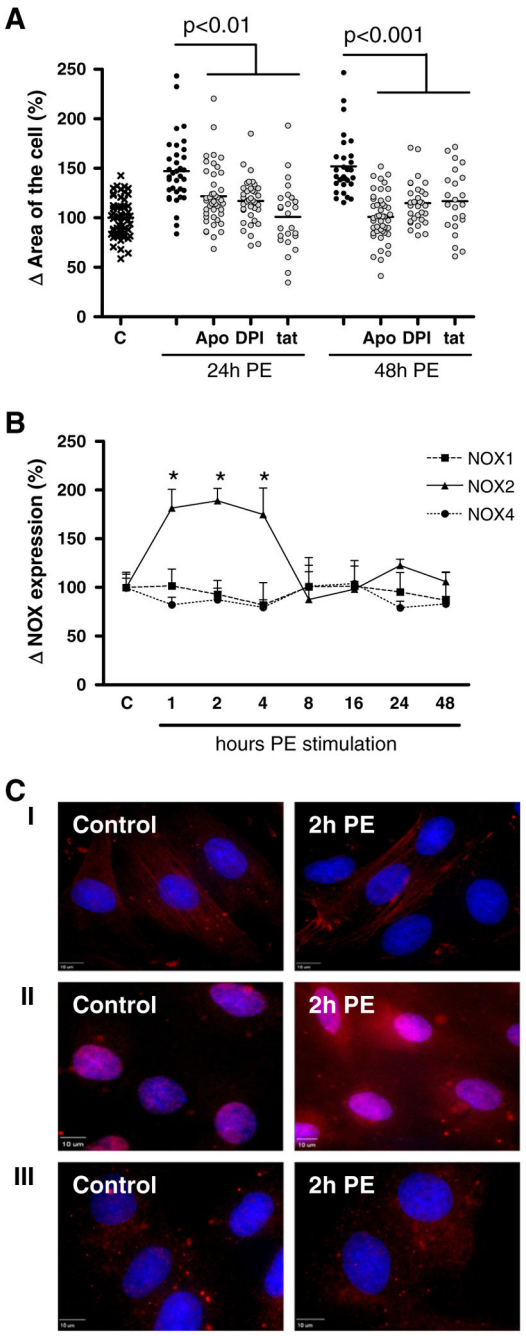

Fig. 2.

Time-dependent role for NOX2 in phenylephrine-induced hypertrophy of H9c2 cells. Digital-imaging microscopy analysis of H9c2 cells at different time points after phenylephrine (PE)-stimulation. (A) Analysis of the effect of apocynin (Apo), diphenylene iodonium (DPI) and NOX2 docking sequence tat peptide (tat) after 24 and 48 h (n = 3). (B) NOX1, NOX2 and NOX4 expression levels (n = 4). The changes are shown as the difference (Δ) in the percentage compared to control cells set to 100%. *p < 0.001. (C) Sub-

cellular localization analysis of NOX1 (I, red signal), NOX2 (II, red signal) and NOX4 (III, red signal). Nuclei are stained with DAPI (blue signal), representative for $n = 4$.

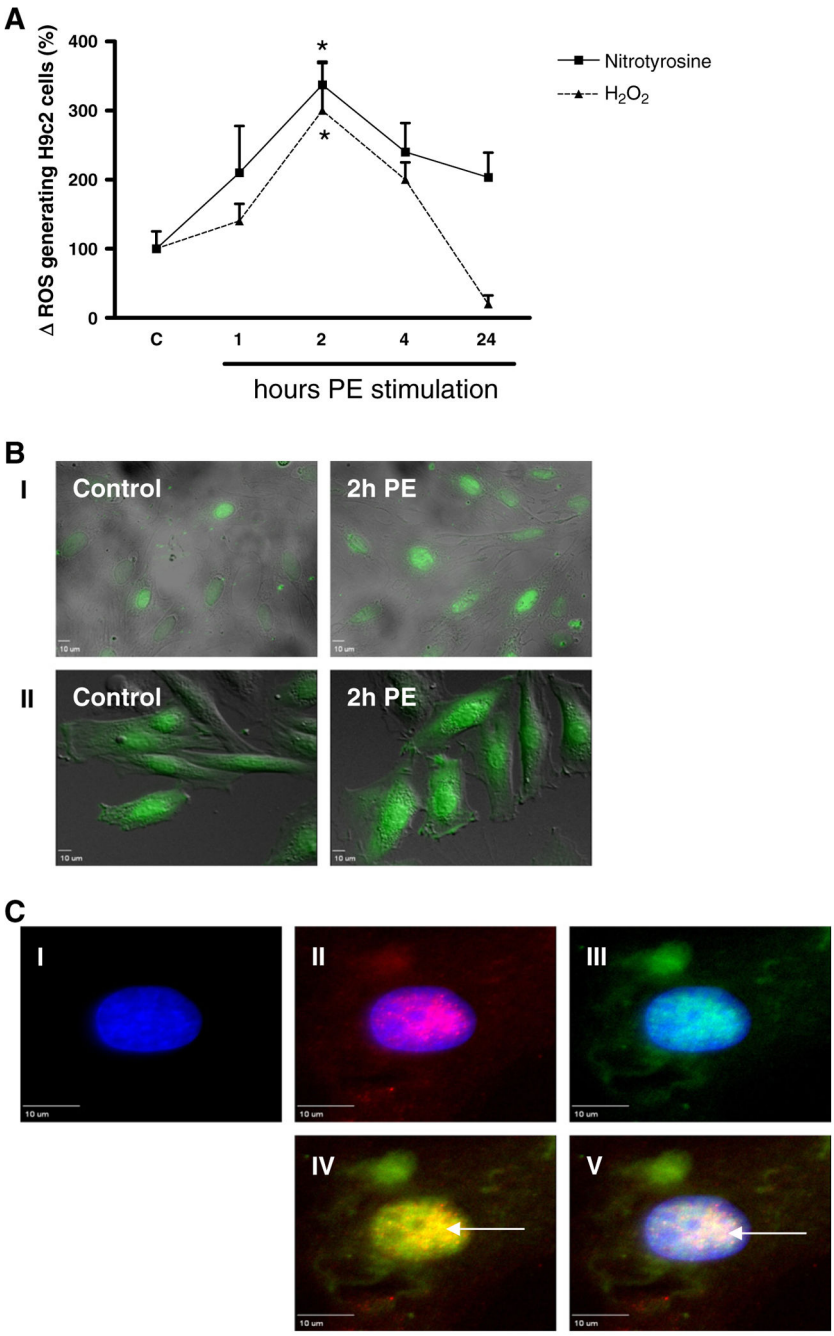

Fig. 3.

Time-dependent subcellular phenylephrine-induced ROS generation in H9c2 cells. Digital-imaging microscopy analysis of phenylephrine (PE)-stimulated H9c2 cells after different time intervals. (A) Cellular ROS levels as measured via nitrotyrosine and H_2O_2 (CM-H_2DCFDA) (n = 3). Changes are shown as the difference (Δ) in the percentage compared to control cells set to 100%. *$p < 0.01$. (B) Subcellular localization analysis of nitrotyrosine (I, green signal) and H_2O_2 (II, green signal), representative for n = 3. (C) Subcellular localization of NOX2 and nitrotyrosine in phenylephrine-stimulated H9c2 cells. Cells were

stained with DAPI (nuclei; I blue signal) and for NOX2 (II, red signal) or nitrotyrosine (III, green signal). Pictures IV and V demonstrate that after 2 h of PE (peri)nuclear NOX2 focally coincides with nitrotyrosine (yellow signal, arrow) and with DAPI (white signal, arrow).

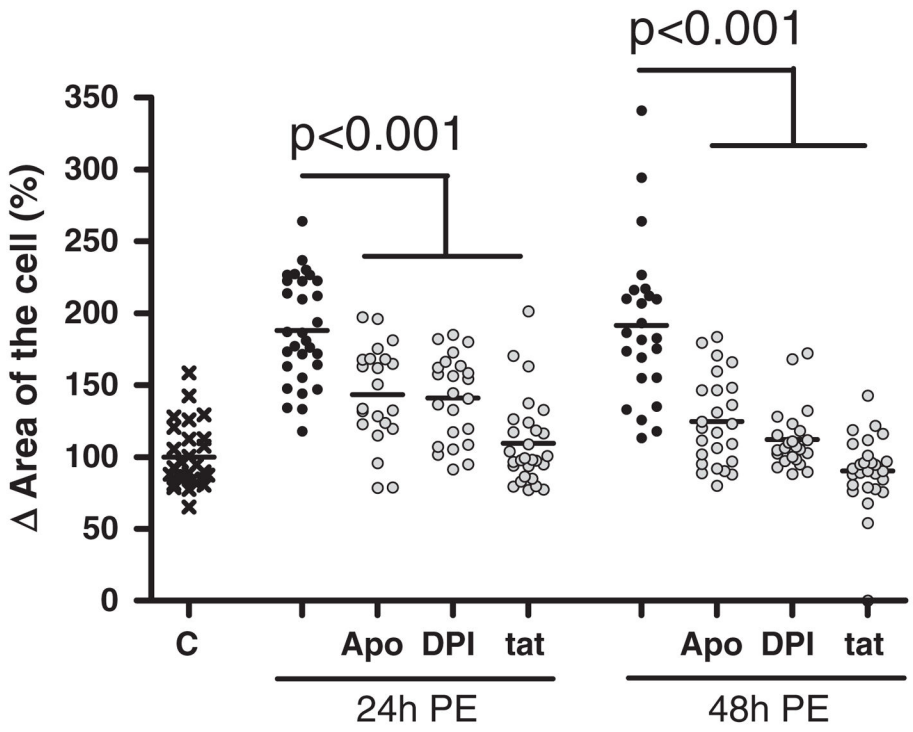

Fig. 4.

Early inhibition of NOX-mediated ROS production decreases phenylephrine-induced hypertrophy. Digital-imaging microscopy analysis of phenylephrine (PE)-induced hypertrophy H9c2 cells to which apocynin (Apo), diphenylene iodonium (DPI) and NOX2 docking sequence tat peptide (tat) were added during the first 4 h only, when stimulated with PE during 24 h and 48 h (n = 3). The changes in cell area are shown as the difference (Δ) in the percentage compared to control cells set to 100%.